

The Influence of Additions in the Use of Glass Fibre Reinforced Cement as a Construction Material

Alejandro Enfedaque, Marcos G. Alberti, Jaime C. Galvez

Department of Civil Engineering: Construction, E.T.S. de Ingenieros de Caminos, Canales y Puertos, Universidad Politécnica de Madrid, Madrid, Spain

Email: jaime.galvez@upm.es

Received 26 November 2015; accepted 2 February 2016; published 5 February 2016

Copyright © 2016 by authors and Scientific Research Publishing Inc.

This work is licensed under the Creative Commons Attribution International License (CC BY).

<http://creativecommons.org/licenses/by/4.0/>



Open Access

Abstract

Although in recent years glass fibre reinforced cement (GRC) has been used in buildings and infrastructure, its application in structural elements has been somewhat restricted due to the worsening of its mechanical properties with ageing and the limited data available related with its fracture energy. With the aim of developing existing knowledge of GRC, the fracture energy in an in-plane and out-of-plane direction of the panel has been obtained. Three types of GRC with different formulations have been tested. The results showed that the fracture energy of a GRC with a 25% addition of a pozzolanic admixture is 40% and 8% higher than a standard GRC in, respectively, in-plane and out-of-plane directions. Similarly, an addition of 25% of thermal-treated kaolin to a standard GRC increases its fracture energy up to 490% and 400%, to the corresponding orientation. The use of digital image correlation (DIC) in the fracture test analysis has permitted a description of the damaging patterns and explanation of the behaviours identified in the fracture tests performed. The multi-cracking process that appears explains the higher fracture energy found in the GRC with an addition of 25% of the aforementioned thermal-treated kaolin. The analysis performed by means of DIC and the results obtained showed GRC with an addition of 25% of thermal-treated kaolin to be the most suitable formulation for possible future structural applications with a short life span in horizontal and vertical elements.

Keywords

GRC, Fracture Energy, Glass Fibre, Digital Image Correlation, DIC

1. Introduction

The remarkable mechanical properties of glass fibre reinforced cement (GRC) have enabled its use as construction

How to cite this paper: Enfedaque, A., Alberti, M.G. and Galvez, J.C. (2016) The Influence of Additions in the Use of Glass Fibre Reinforced Cement as a Construction Material. *Materials Sciences and Applications*, 7, 89-100.

<http://dx.doi.org/10.4236/msa.2016.72009>

material in numerous architectural and civil engineering applications. It has been profusely employed in cladding panels, telecommunication towers, sewers and, among others, permanent formworks [1]-[4]. This variety of application has been achieved due to its lightness and the versatility of shaping that it can adopt due to an absence of steel bar reinforcement.

However, in almost all the aforementioned uses, the load bearing capacity that the fibres provide to the composite material is not considered in the structural design. The latter is justified because previous published research has shown that the ductility and enhancement of the mechanical properties that the glass fibres provide to the construction material are diminished as time passes [5]-[8]. This problem, which is commonly known as GRC ageing, has been studied thoroughly and some researchers have shown that its main cause is the corrosion of the glass fibres in the highly alkaline environment of the cement paste [9].

While there have been attempts to reduce the harmful influence of cement matrix alkalinity by adding chemical products such as silica fume, metakaolin or acrylic resins to the cement mortar [10] [11], no definitive results have been obtained. In addition, as in the event of cracking there is no reinforcement that can absorb the bearing loads it is important to determine the ductility of GRC. Moreover, assessment of the influence of the additions previously cited in the fracture energy would be a key design parameter for future applications in the short term. By obtaining these results, short-term and long-term applicability of GRC as a construction material for structural elements could be drastically extended.

This study assessed the fracture energy of three different types of GRC: a standard GRC and two GRC with chemical additions. The behaviour of GRC in the two most common orientations of the fibres when used in construction elements was obtained. In addition, the fracture processes were analysed by using digital image correlation (DIC) synchronized with the fracture tests, developing existed knowledge about the behaviour of GRC in the day-to-day construction elements [1]. The results showed that a high content of metakaolin addition induces changes in the damage mechanisms that occurred in both orientations of GRC, enabling a multi-cracking process that enhanced fracture energy and ductility.

2. Test Programme

2.1. Material Production and Sample Preparation

A test programme was carried out with GRC samples manufactured with three distinct formulations. In two of these formulations, two chemical products were employed: Powerpozz[®] and Metaver[®]. Powerpozz[®] is a pozzolanic admixture, while Metaver[®] is a thermal-treated pure kaolin. The compositions of the chemical additions can be seen in **Table 1** [12] [13]. The components and content used in GRC production can be observed in **Table 2**.

The test boards were manufactured with approximate dimensions of 1200 mm in length, 1200 mm in width and 10 mm in thickness approximately. They were produced by simultaneous projection of cement mortar and

Table 1. Centesimal composition of chemical additions.

	Powerpozz [®]	Metaver [®]
SiO ₂	52 - 55	52 - 54
Al ₂ O ₃	41 - 44	40 - 42
Fe ₂ O ₃	<1.90	<2.5
TiO ₂	<3	<1.0
SO ₄	<0.05	-
P ₂ O ₅	<0.2	-
CaO	<0.2	<0.5
MgO	<0.1	<0.4
K ₂ O	0.75	<2.0
Na ₂ O	--	<0.1
LOI	<0.50	Not declared

Table 2. Cement mortar formulations.

	Cement (kg)	Sand (kg)	Water (kg)	Plasticizer (l)	Addition (kg)
Control GRC	50	50	17	0.5	-
GRC with Metaver [®] (GRC-M)	50	50	23	0.5	12.5
GRC with Powerpozz [®] (GRC-P)	50	50	25	0.5	12.5

chopped 38 mm-long glass fibres, using the same process as that commonly used in GRC industry. The volumetric fraction of fibres was around 5% which, as previously stated, is the best option to improve the mechanical behaviour of GRC [9]. The orientation of the glass fibres is predominantly orthotropic, with the fibres being almost parallel to the two main dimensions of the board.

After 24 hours, the test boards had set. They were then demoulded and taken to a climatic chamber with 20°C and 98% of humidity. After 28 days, the boards were removed from the climatic chamber and stored in a laboratory environment until testing.

A frame of 50 mm, near the edges of the board, was cut and discarded to avoid testing GRC samples with bent fibres, which are typically placed in such removed borders. From each test board six rectangular 178 × 55 mm² samples were cut. In order to obtain comparable results, the surface of the samples was evened by means of a refrigerated grinder until the same thickness was reached.

The fracture tests were carried out in two orientations: one with the fibres parallel to the loading direction (in-plane of the panel direction) and one with the fibres perpendicular to the loading direction (out-of-plane of the panel direction). Accordingly, the samples were notched by using two processes. Those that were tested in a perpendicular direction to the fibres (**Figure 1(a)**) were machined to obtain a notch 1 mm wide. The depth of this notch was 3 mm and was made parallel to the board. In addition, the specimens tested in the parallel direction (**Figure 1(b)**) were notched by using a three-millimetre thick circular saw. An 18 mm notch normal to the main two directions of the test board was made in this type of sample. In both orientations, the notch was a third of the total cross section.

2.2. Test Setup

Among the many applications of GRC in the building industry there are certain uses where the fibres are almost parallel to the loading direction, such as façade panels. However, there are other usages—such as permanent formwork—where the fibres are perpendicular to the loading direction. The properties in both orientations have been previously studied by performing different types of tests, such as the four-point bending tests [14]. However, at the time of writing there has been not enough published data available about the fracture energy of GRC in any orientation.

The process carried out to assess the fracture energy of GRC was based on the recommendations for obtaining the fracture energy of concrete, which have been extensively used with successful results [15] [16]. When adapting the recommendation RILEM TC-187-SOC to GRC, the relation between the dimensions of the samples could not be maintained due to a reduced thickness. It is worth noting that if the thickness of the GRC were increased, one of the main advantages of GRC (that is to say, its reduced weight) would disappear. However, the rest of suggestions have been followed.

Tests in in-plane and out-of-plane directions were performed in a universal testing machine equipped with, respectively, a 10 kN and 1 kN load cell. The test instrumentation involved two linear variable differential transformers (LVDT) placed at both sides of the samples and a crack mouth open displacement (CMOD) strain gauge. The latter was fixed to the notch lips by using a pair of steel blades glued to the samples. The data acquisition system of the testing machine registered the CMOD, the deflection detected by the LVDT sensors and data acquired by the load cell. In addition, the position of the machine actuator was also obtained. All tests were controlled by the CMOD gauge opening velocity at a reduced speed. The latter ensured a stable cracking process.

In addition to the aforementioned data, a two-dimensional DIC system was employed to analyse the fracture process. In order to perform the numerical analysis of the images recorded, it was necessary that the surface of

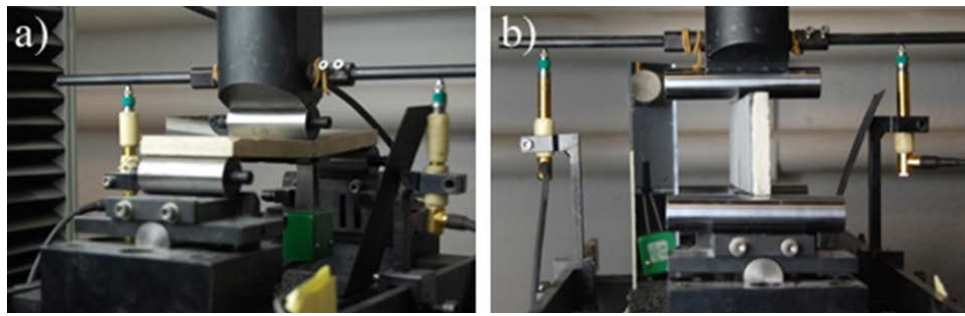


Figure 1. Test setup: (a) perpendicular to fibres; (b) parallel to fibres.

the specimen had a speckle grey distribution that deformed along with the material. This texture was obtained in the GRC samples by painting them black and spraying on their surfaces a white-dotted pattern.

The camera employed to record the test is usually placed perpendicular to the sample. However, in these tests this disposition could not be employed due to the presence of LVDT at both sides of the sample, as can be seen in **Figure 1**.

With the aim of overcoming problem, it was decided to record the test using a mirror oriented at 45° of the sample and the camera alike. The camera setup can be seen in the sketch shown in **Figure 2**. Moreover, in **Figure 1(b)** the aforementioned mirror and the two LVDT gauges may be seen. A more detailed description can be found in previous studies [17].

3. Results and Discussion

3.1. Fracture Tests in an Out-of-Plane Direction

Preparation of the average load-CMOD curves has been carried out in order to compare the results obtained in the tests performed when introducing the load in a perpendicular direction. These curves can be seen in **Figure 3**.

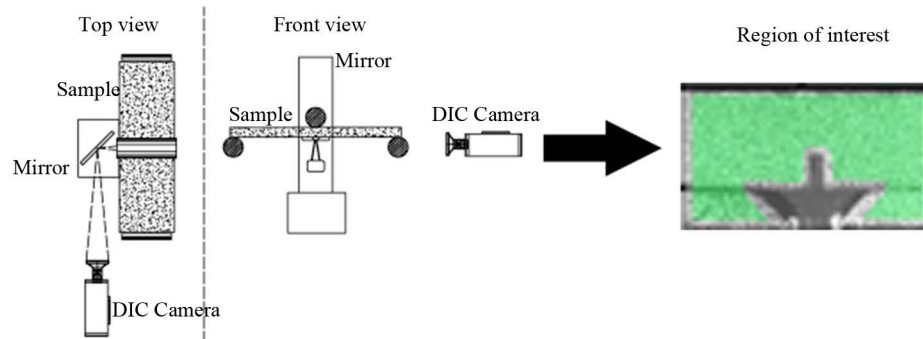
The average behaviour of the three GRC samples tested in a normal orientation without any additive can be seen in **Figure 3**. No remarkable scattering was found in any of the three tests performed. It is worth noting that the shape of the curve is similar to those obtained in the fracture tests of concrete specimens [16]. There are two clearly identified zones. The first zone is linear up to the limit of proportionality (LOP). The second zone, after this point, is a stable cracking branch that ends when the maximum load is reached. The curve in the unloading branch takes the shape of an exponential softening function.

Similarly to the curves of the samples of GRC without additions, the shape of the GRC-M plot resembles the fracture curve of concrete. There was almost no scattering in the results of these three samples. In addition, the behaviour can be divided in two main zones: a linear loading branch and an unloading branch. However, in these curves the LOP was also the point of maximum load. There was no increment of the bearing capacity of the material after this LOP was reached. This zone was then followed by a branch with a slow unloading process that also resembled an exponential curve. The final crack opening in these tests was close to 4 mm in the cases of load values similar to the preload ones being registered.

Regarding the GRC-P curves, moderate scattering appeared both in the loading and unloading part of the test curves. The LOP was not particularly distinguished in the curves because there was a continuous increment of the flexibility of the samples while the load was still increasing. Although the unloading process of the samples registered some degree of scattering, there were some trends identified that merit mention. Given that there was an almost constant reduction rate of the bearing capacity of the samples during the unloading part of the test, this part resembled more a bilinear or a straight line than an exponential function. When the upper boundary of the CMOD was reached, approximately at 4 mm, the samples withstood a load greater than the preload value. The last CMOD registered corresponded to the upper limit of the gauge.

Figure 3 shows noticeable differences in the peak load that the materials can bear, with GRC being the highest (around 120 N). GRC-P samples withstood a load slightly above 100 N, while GRC-M samples resisted around 95 N. It is important to highlight that the maximum load was reached in GRC and GRC-P samples after the limit of proportionality (LOP) had been exceeded. The GRC and GRC-P samples, consequently, suffered a

Tests perpendicular to fibers



Tests parallel to fibers

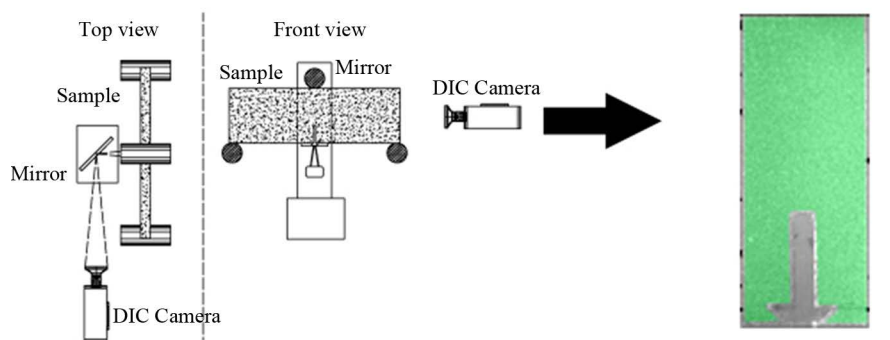


Figure 2. Video camera setup.

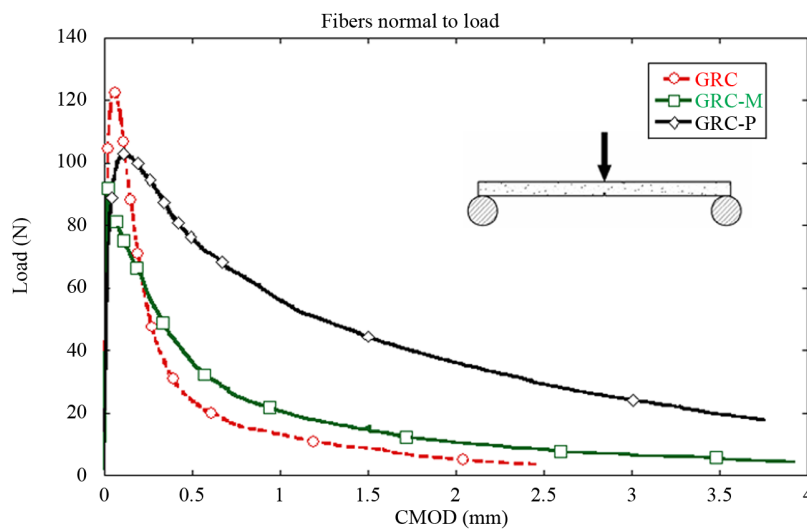


Figure 3. Average behaviour of the three types of materials studied. Fibres are perpendicular to the load.

loss of stiffness between the LOP and the maximum load. However, the behaviour of the GRC-M samples was elastic and linear up to the LOP. The different behaviour of the materials meant that the CMOD where the maximum load occurs changed for all the formulations. Among them, the greatest values corresponded to GRC-P samples.

The behaviour differences described in the previous paragraph can be quantified by using the work that entails fracturing the samples and obtaining the fracture energy of the three formulations studied. The fracture energy was obtained by dividing the fracture work by the fractured area. The results can be seen in **Table 3** as well as the coefficient of variation (c.v.) obtained for each formulation.

Table 3 shows that the fracture energy of GRC is the lowest of the three formulations used. The GRC-M and GRC-P fracture energies are, respectively, 141% and 486% greater than the GRC one.

To analyse the relation between the curves obtained in the tests and the damaging mechanisms that appear during such tests, the strain fields at maximum load and at $CMOD = 0.5$ mm were obtained by means of DIC. These images can be seen, respectively, in **Figure 4** and **Figure 5**.

Figure 4 shows significant differences in the horizontal strain component of the three formulations. In order to make a valuable comparison, the three images were obtained by using the same colour scale values. In the image of the GRC-M and GRC without additions, the samples showed a limited zone of concentration of damage. This can be identified by comparing the green areas, which corresponded to low strains, with those that gathered the damage (the strains that appear are shown in reddish tones). In the image taken of a GRC-P sample, a strain concentration in the notch tip can be clearly seen. There is a red coloured spike that begins at the notch tip and ends near the middle of the ligament. Therefore, it appears that GRC-P is capable of distributing the damage produced in the test into wider regions of the ligament. By relating the loss of stiffness and the strain concentration, it can be deduced that in the red coloured zone one or more cracks might have appeared.

The damaging patterns that appear in the samples when the $CMOD$ was equal to 0.5 mm can be seen in **Figure 5**. In this figure, the same trends as those previously described for **Figure 4** are confirmed. The area where

Table 3. Fracture work and energy of the three types of materials studied in tests in out-of-plane direction.

	Fracture work (Nmm)	Fracture energy (N/m)	c.v.
GRC	147.9	441.6	0.05
GRC-M	175.9	620.9	0.14
GRC-P	641.5	2148.7	0.05

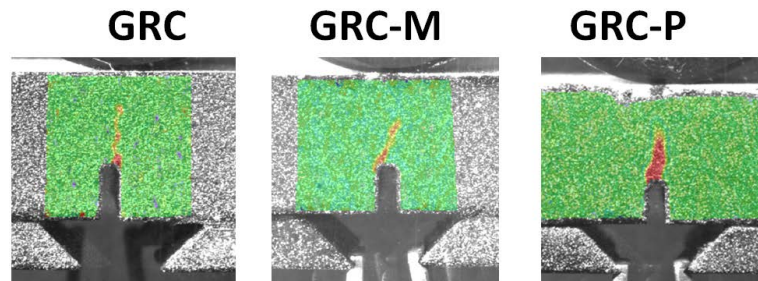


Figure 4. Strain distribution at maximum load (fracture tests in an out-of-plane direction).

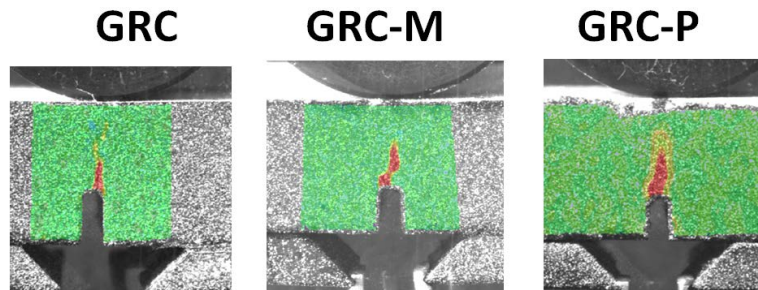


Figure 5. Strain distribution at $CMOD = 0.5$ mm (fracture tests in an out-of-plane direction).

the damage produced by the loading cylinder when moving downwards is noticeably wider in the GRC-P samples than in the other two formulations. However, and in contrast to what happened at the maximum load, some differences can be noted between GRC and GRC-M. It is clear that in the case of GRC-M the damaged area is vaster than in the GRC without additions. Moreover, when the load-CMOD curves shown in **Figure 3** are compared with **Figure 4** and **Figure 5**, the enhancement of the load bearing capacity at a certain CMOD seems to be related with the area where the damage was concentrated.

In order to quantify the differences in ductility of the three formulations studied, a crack opening displacement (COD) analysis was performed as a complement to the strain field analysis of **Figure 4** and **Figure 5**. The COD was measured by using DIC. **Figure 6** offers a comparison of the effects of the additions used in the material ductility. This figure shows the relative values of COD at the notch tip at the different load stages studied for the three formulations used. The COD of GRC was used as a reference and appears in the figure as 100% in every loading stage analysed. As can be seen, the GRC-M has a greater ductility than GRC, though only in the last part of the test. Only when the load was lower than 40% of the maximum load during unloading did the GRC-M samples have a greater ductility than the GRC. However, the GRC-P samples were more ductile than GRC throughout the fracture test. The greatest values were found at the end, as could be expected, when analysing the fracture tests.

3.2. Fracture Tests in an In-Plane Direction

In order to compare the results obtained in the tests performed by placing the load in a parallel direction to the sample surface, the average load-CMOD curves were prepared. These curves can be seen in **Figure 7**.

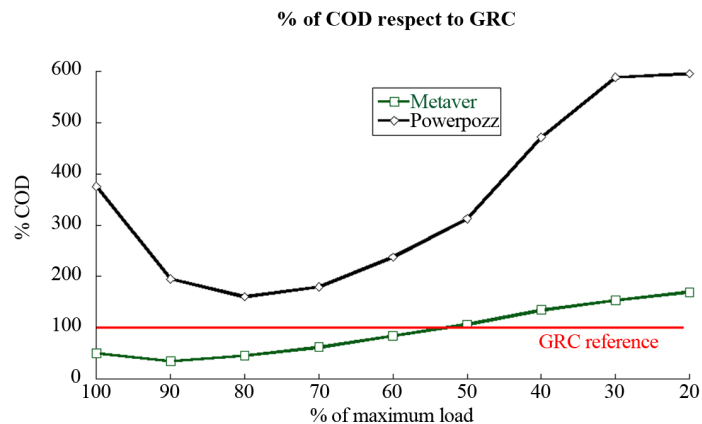


Figure 6. Relative COD at notch tip. 100% correspond to GRC. COD at that loading point.

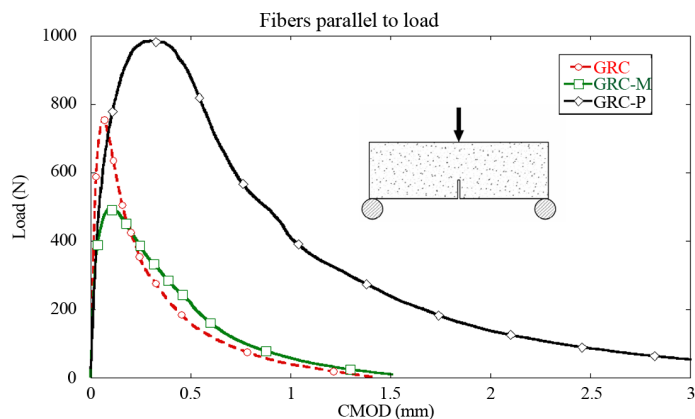


Figure 7. Average behaviour of the three types of materials studied. Fibres are parallel to the load.

In the tests performed with GRC specimens without additions, there was hardly any scatter in the three tests performed. The shape of the average curve obtained was similar to the fracture behaviour of concrete. There was a linear loading branch followed by a soft unloading branch. This zone could be compared to an exponential function. In such a case, the LOP and the maximum load almost coincided with there being only minor changes of stiffness between the LOP and the maximum load. The opening of the crack when the samples failed was, in all the tests, close to 1.5 mm.

The results of the fracture tests performed on GRC-M and the fibres parallel to the load had the same characteristics as those previously mentioned in the case of GRC without additions. There were scarcely any differences between the behaviour of each of the three samples tested. The unloading branch of the curve showed a more gradual unloading process. This was highly noticeable directly after the maximum load. In this area, the material withstood the load while the sample lost a significant part of its stiffness and the opening of the notch increased. Immediately after this, the unloading process developed at a constant rate until there was a final change of curvature when CMOD was 0.65 mm. After this point, the behaviour of the samples began to unload with an exponential shape until a CMOD of 1.5 mm was registered when the samples collapsed.

The fracture tests performed in the GRC-P samples showed, as in the other orientation studied, some degree of scattering. Nevertheless, some trends could be described. There were three areas in which the curves could be divided. The first zone was linear elastic and ended with the LOP way before reaching the maximum load. Until this point, the behaviour of each of the samples was almost equal. Afterwards, in the second zone, given that the loss of stiffness of the samples began the slope of the curves decreased. Nonetheless, the load still grew, causing greater strains in the samples. This increment in load continued until the maximum load was reached and the unloading process started. There were slight differences in the CMOD registered at the same load for the samples. This area ended when a CMOD of 1.5 mm was reached. Conversely, when the third zone began, the samples behave similarly, with the test curves showing a similar slope and ending when the CMOD reached 3 mm. At this point, the loads registered were greater than the preload.

Comparing the GRC average maximum loads, while the GRC-P reaches a load 35% higher than GRC the GRC-M was only 65% of that of GRC. The LOP was in all the formulations significantly lower than the maximum load. Therefore, there was a reduction of stiffness of the samples while the load bearing capacity was still increasing. These differences were also noticeable in the CMOD at the maximum loads of the three formulations. By analysing the unloading parts of the average curves, it can be observed that for the three types of GRC followed a soft unloading and had an exponential shape.

Another factor that should be highlighted is that the ductility of the GRC and GRC-M was similar, as can be observed in the CMOD at failure while GRC-P samples were beyond 200% more ductile. The failure CMOD was greater than 3 mm. This was a remarkable value, given the height of the samples tested (55 mm).

The fracture energy in an in-plane and out-of-plane direction of the panel was obtained by following an analogue process such as that used in the perpendicular tests. The values found can be seen in [Table 4](#) together with their coefficient of variation. This table shows that the fracture energy of the GRC-M samples was only 7% higher than GRC. On the contrary, the GRC-P samples had a fracture energy of 400% higher than GRC.

In order to analyse the relation between the curves obtained in the tests and the damaging mechanisms that appeared during the tests, the strain fields at maximum load and at CMOD = 0.6 mm were obtained by means of DIC. These images can be seen, respectively, in [Figure 8](#) and [Figure 9](#).

[Figure 8](#) shows the strain field at maximum load for the three formulations studied. The colour scale is specified as equal in all the images to enable a comparison between each one. The green zones that appear in [Figure 8](#) correspond to the areas with low strains, while the reddish areas correspond to higher strains. According to this, the GRC samples analysed showed a crack with an origin at the notch and bound to the upper part of the sample

Table 4. Fracture work and fracture energy of the three types of materials studied in tests with in-plane direction.

	Fracture work (Nmm)	Fracture energy (N/m)	c.v.
GRC	167.4	456.6	0.07
GRC-M	180.0	490.8	0.03
GRC-P	669.1	1824.8	0.01

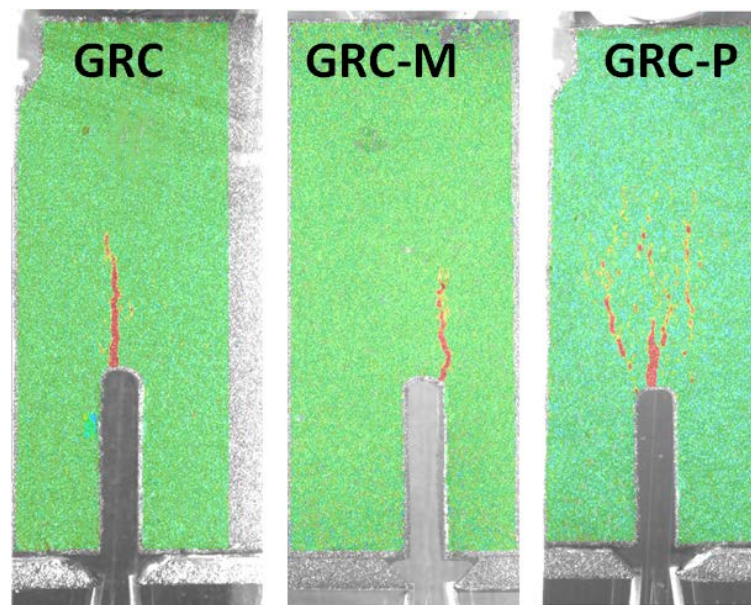


Figure 8. Strain distribution at maximum load (fracture tests in an in-plane direction).

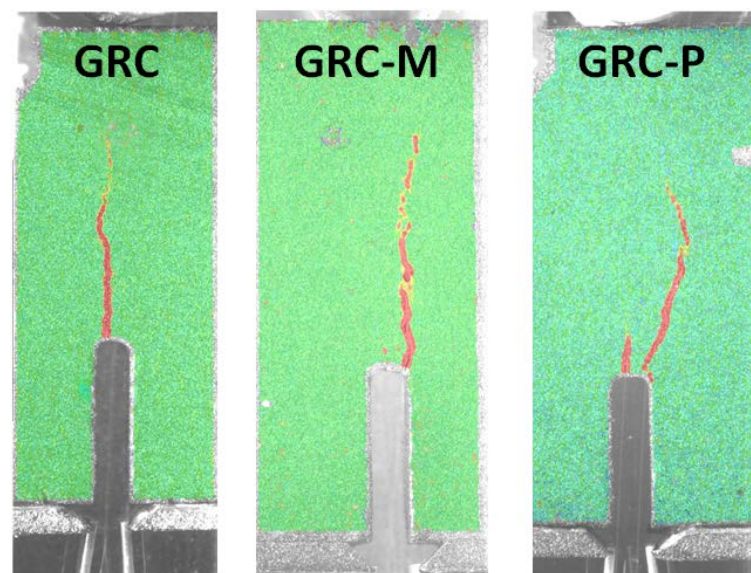


Figure 9. Strain distribution at CMOD = 0.6 mm (fracture tests in an in-plane direction).

where the load was applied. Regarding the GRC-M sample, instead of having only one crack, there were a few cracks with smaller openings that grew from the top of the notch. However, there was one crack that concentrated most of the strain and started in the right part of the notch. The CMOD values registered at maximum load were similar in both formulations. Therefore, the addition of the openings of the group of cracks of the GRC-M sample was similar to the opening of the only crack that appeared in the GRC sample. Nonetheless, the CMOD at maximum load of GRC-P was significantly greater than in the two formulations previously mentioned. This was caused by the amount of the cracks that appeared before reaching the maximum load. In the GRC-P sample, the group of cracks was clearly developed with some of them reaching the half of the ligament.

As can be clearly seen in **Figure 8**, the GRC-P samples showed multi-cracking. The principal crack diverts from the top of the notch, while the others appear at both sides of the latter. This group of cracks caused the loss

of stiffness than can be observed in the load-CMOD curve.

Figure 9 shows the cracking process of a GRC sample. Each image shows the formation of the final fracture. By comparing the image that corresponds to the GRC in **Figure 8** and that of GRC in **Figure 9**, it is clear that the fracture process could only be attributed to the occurrence and progress of only one cracking area. The initial crack that appeared when the maximum load was reached grew towards the upper part of the ligament when CMOD was equal to 0.6 mm. A similar process occurred in the fracture test of a GRC-M sample. According to the data registered and analysed by DIC, there was no evidence of multi-cracking. The crack that appeared in the right part of the notch in the loading part of the test developed, as the test progressed, towards the application point of the load. In contrast to what took place in the GRC and GRC-M samples, the GRC-P sample fractured by means of another damage mechanism. When the maximum load was reached, there were a few independent cracks opening simultaneously. The crack that was initiated in the first place grew and widened towards the loading point, though some others appeared in the left and right part of the ligament area. In the image shown in **Figure 9**, it can be perceived how a crack appeared in the right part of the ligament zone and how it developed towards the loading point (thus creating the final fracture of the material). Simultaneously, the rest of the cracks that had appeared began to close as the final fracture progressed. In addition, the initial crack that appeared in the centre part of the notch closed as the test progressed while the final fracture was growing.

To quantify the influence of multicracking behaviour of the GRC-P samples with respect to the GRC and GRC-M sample, a measurement of the COD of the cracks during the test was performed. The COD of the three types of materials tested can be seen in **Figure 10**. The COD values shown correspond to the addition of the opening of all the cracks in the ligament zone. The COD of GRC has been used as reference and appears in the figure as 100% in every loading stage analysed. From the beginning of the test, the GRC-P sample bore a COD of at least 200% higher than GRC, with it being during most of the test more than 300% greater (as **Figure 10** shows). Conversely, the GRC-M was stiffer when 50% of the maximum load was applied and cracking had not occurred. After this point, the ductility of the GRC-M sample was at least 140% greater than the GRC sample.

4. Conclusions

The fracture energy of GRC was assessed by means of a new approach based on the recommendations for conventional concrete. The testing techniques included the supplementary support of DIC methods. The fracture energy was obtained in orientations in-plane and out-of-plane direction of the panel. With the use of chemical additions to conventional GRC, the results showed enhancements in toughness and ductility compared with GRC.

In the case of Metaver[®], 25% of addition slightly increased the fracture energy of GRC in-plane direction, while in out-of-plane direction this increment was remarkable. When using 25% of addition of Powerpozz[®], the fracture energy of a normal formulation of GRC was quadrupled when compared with the fracture energy of GRC. This occurred in the two tested directions, in-plane and out-of-plane direction of the panel.

The use of DIC allowed multi-cracking evidence to be visualized. Such an effect would increase fracture

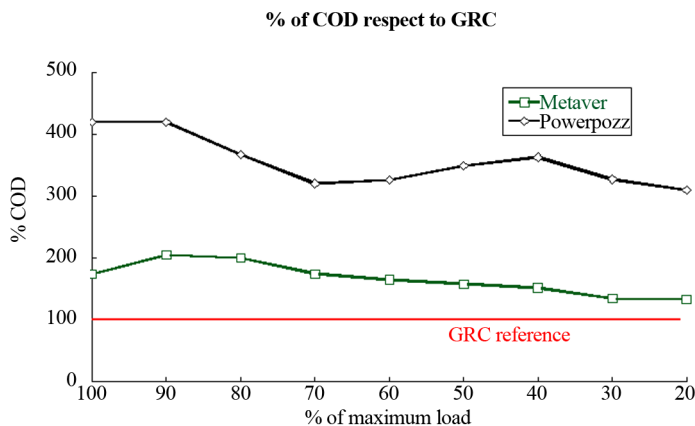


Figure 10. Relative COD at notch tip. 100% correspond to GRC. COD at that loading point.

energy. There was no multi-cracking response in any of the materials tested in out-of-plane direction of the panel.

Nevertheless, in the parallel direction image processing allowed the identification of two damage mechanisms. The GRC and GRC-M specimens showed a limited capacity to redistribute damage within the cross section. The crack growth in such specimens occurred from the development of only one initial single and hairline crack which, at the end, crossed the sample height. However, the tests with the GRC-P specimens showed that several cracks could develop and grow, even reaching areas of up to half the height of the section. Only one of the cracks produced the final failure when crossing the whole section. The rest of the cracks closed in such advanced deflections. These multi-cracking mechanisms increased the energy needed to produce the fracture and, therefore, significantly increase the values of fracture energy. The DIC analyses permitted localizing this effects and finding that such increment is caused by the opening and closing of few additional cracks.

The fracture energy obtained in the two orientations was compared for each formulation and the results were analogous. Only GRC-M showed some differences, probably due to the diverse fracture mechanisms involved in the fracture processes.

The results obtained and the analysis performed by means of DIC showed GRC-P as the most suitable formulation for possible future structural applications. Such a formulation behaved with remarkable ductility in both orientations, widening its use not only in vertical elements (such as façade panels) but also in horizontal elements (such as permanent formwork). The test results suggest that a more detailed study of the possible structural uses of this material could be considered in examining structural elements with a limited life span.

Acknowledgements

The authors gratefully acknowledge the financial support provided by Ministry of Economy and Competitiveness of Spain by means of the Research Fund Project DPI 2011-24876. They also offer their gratitude to the Materials Science Department of the Technical University Madrid for supplying the DIC device.

References

- [1] Ferreira J.G. and Branco, F.A. (2007) Structural Application of GRC in Telecommunication Towers. *Construction and Building Materials*, **21**, 19-28. <http://dx.doi.org/10.1016/j.conbuildmat.2005.08.003>
- [2] Kim, G.B., Pilakoutas, K. and Waldron, P. (2008) Development of thin FRP Reinforced GFRC Permanent Formwork Systems. *Construction and Building Materials*, **22**, 2250-2259. <http://dx.doi.org/10.1016/j.conbuildmat.2007.07.029>
- [3] Shah, S.P., Ludirdja, D., Daniel, J.I. and Mobasher, B. (1988) Toughness Durability of Glass Fiber Reinforced Concrete Systems. *ACI Materials Journal*, **85**, 352-360.
- [4] Correia, J.R., Ferreira, J. and Branco, F.A. (2006) A Rehabilitation Study of Sandwich GRC Facade Panels. *Construction and Building Materials*, **20**, 554-561. <http://dx.doi.org/10.1016/j.conbuildmat.2005.01.066>
- [5] Grutzeck, M.W. (1981) Advances in Cement-Matrix Composites Proceedings. Materials Research Society, 102C Materials Research Laboratory, University Park, PA.
- [6] Majumdar, A.J. (1975) Fiber Reinforced Cement and Concrete. Construction Press, Forestville, 279-314.
- [7] Mobasher, B. and Shah, S.P. (1989) Test Parameters for Evaluating Toughness of Glass Fiber Reinforced Concrete Panels. *ACI Materials Journal*, **86**, 448-458.
- [8] Shah, S.P., Ludirdja, D., Daniel, J.I. and Mobasher, B. (1988) Toughness-Durability of Glass Fiber Reinforced Concrete Systems. *ACI Materials journal*, **85**, 352-360.
- [9] Majumdar, A.J. and Laws, V. (1991) Glass Fiber Reinforced Cement. BSP Professional Books, Oxford.
- [10] Marikunte, S., Aldea, C. and Shah, S.P. (1997) Durability of Glass Fiber Reinforced Cement Composites. *Advanced Cement Materials*, **5**, 100-108. [http://dx.doi.org/10.1016/S1065-7355\(97\)00003-5](http://dx.doi.org/10.1016/S1065-7355(97)00003-5)
- [11] Enfedaque Díaz, A., Sánchez Paradela, L. and Sánchez-Gálvez, V. (2010) The Effect of Silica Fume and Metakaolin on Glass-Fibre Reinforced Concrete (GRC) Ageing. *Materiales de Construcción*, **60**, 67-82.
- [12] Metaver. http://catalogue.newchem.org/finlandstore/Up_files%5CMD5%20Metaver%20I.pdf
- [13] Powerpazz. http://www.bigfreshcontrol.com/documents/act_documents/10.150MetakaolinPhys&ChemWhite.pdf
- [14] Enfedaque, A., Paradela, L.S. and Sánchez-Gálvez, V. (2012) An Alternative Methodology to Predict Aging Effects on the Mechanical Properties of Glass Fiber Reinforced Cements (GRC). *Construction and Building Materials*, **27**, 425-431. <http://dx.doi.org/10.1016/j.conbuildmat.2011.07.025>

- [15] Enfedaque, A., Romero, H.L. and Gálvez, J.C. (2014) Fracture Energy Evolution of Two Concretes Resistant to the Action of Freeze-Thaw Cycles. *Materiales de Construcción*, **64**, e005. <http://dx.doi.org/10.3989/mc.2014.00813>
- [16] Fathy, A.M., Sanz, B., Sancho, J.M. and Planas, J. (2008) Determination of the Bilinear Stress-Crack Opening Curve for Normal- and High-Strength Concrete. *Fatigue & Fracture of Engineering Materials & Structures*, **31**, 539-548. <http://dx.doi.org/10.1111/j.1460-2695.2008.01239.x>
- [17] Enfedaque, A., Gálvez, J.C. and Suárez, F. (2015) Analysis of Fracture Tests of Glass Fibre Reinforced Cement (GRC) Using Digital Image Correlation. *Construction and Building Materials*, **75**, 472-487. <http://dx.doi.org/10.1016/j.conbuildmat.2014.11.031>